

**THE INFLUENCE OF ACOUSTIC NONLINEARITY ON ABSORPTION
PROPERTIES OF HELMHOLTZ RESONATORS
PART II. EXPERIMENT**

M. MEISSNER

Polish Academy of Sciences
Institute of Fundamental Technological Research
(00-049 Warszawa, Świętokrzyska 21, Poland)
e-mail: mmeissn@ippt.gov.pl

An experimental study of an effect of the acoustic nonlinearity on absorption properties of Helmholtz resonators is presented in this work. By use of the classical standing wave method the changes in the absorption coefficient and the resonators impedance were investigated at moderate and high amplitudes of incident wave. As a result of nonlinearity a high absorption at resonance frequencies was observed and then a decrease in this absorption with increasing amplitude. Measurements of the total loss resistance of resonators have indicated that a change in the resistance at high amplitudes depends strongly on resonator orifice area, the smaller area — the higher increase in the resistance. The experimental results have also shown a growth in resonators reactance which causes an increase in resonance frequency. Quite a good agreement between experimental data and the theory presented in Part I was found.

1. Introduction

Helmholtz resonators have been studied extensively, primarily due to their use in a large number of practical applications. They are effective in a narrow frequency range centered by a resonance frequency and are therefore used to absorb sound at selected frequencies, e.g. in enclosed spaces [1], aircraft cabins [2] and panel systems [3, 4]. In order to develop a rational design procedure for the resonators it is important to investigate their acoustic properties in a wide range of sound intensities.

The case of high intensity sound is of special interest, when a resonator absorption depends on the amplitude of driving pressure due to nonlinear behaviour of orifice impedance. The change in absorption properties of Helmholtz resonators has the following physical explanation. At high amplitudes of excitation, there is a strong acoustic motion through the resonator orifice. It results in a separation of boundary layer and a formation of vortex on the outflow side of the orifice. The vortex moves away from the orifice and due to the viscous action its kinetic energy is ultimately dissipated as heat. The part of acoustic energy, which was transferred to the vortical field, represents an additional energy loss to the resonant system.

In the past a number of workers have studied the acoustic properties of Helmholtz resonators at a high intensity sound. INGARD [5] and BIES and WILSON [6] reported measurements of real and imaginary part of the orifice impedance, while WU and RUDNICK [7] presented experimental data showing a variation in a resonance frequency with increasing sound intensity. CZARNECKI [8, 9] investigated an influence of the nonlinear properties of Helmholtz resonators on acoustic conditions in enclosures. He found an increase or a decrease in the absorption coefficients depending on the conditions of the resonator surroundings.

A purpose of the second of two companion papers is a comparison between results of measurements of acoustic properties of Helmholtz resonators at moderate and high amplitudes, and theory presented in Part I [10]. The experiments were performed by using the standing wave apparatus with cylindrical tube which had a diameter $2a$ (Fig. 1). The resonators placed at the end of this tube were terminated at one end, by a rigid plate with a centrally located circular orifice with a diameter of $2b$ and thickness d , while at the other end by a rigid wall. The resonators dimensions were much less compared with a length of the incident wave.

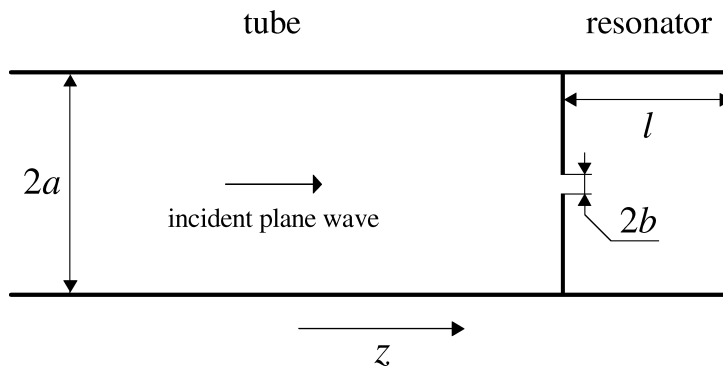


Fig. 1. Helmholtz resonator placed on one end of a tube.

2. Theoretical background

The theory pertaining to the nonlinear absorption properties of Helmholtz resonators has been presented with full particulars in Part I [10]. It has shown that changes in absorption coefficient at high amplitudes are associated with losses resulting from the conversion of the acoustic energy into the vortical energy. In the impedance model of resonator these losses were described by the nonlinear orifice resistance R_n given by the expression

$$R_n = \frac{\rho V_0}{2.46 \pi b^2} \left(\frac{1}{C_c} - \frac{b^2}{a^2} \right)^2, \quad (1)$$

where V_0 is the amplitude of a fundamental component of orifice velocity and C_c is the contraction coefficient which is approximately equal to 0.61 in the case of sharp-edged orifice. Due to the fact that resistance R_n is proportional to the velocity amplitude,

the losses associated with the transfer of the acoustic energy to the vortical field are dominant at very high amplitudes of a driving pressure. If, however, the amplitudes of the pressure are moderate, we must also include in the impedance model of resonator a resistance connected with a viscous damping inside the resonator orifice. According to INGARD [5], this resistance can be described by the following empirical formula

$$R_\mu = \frac{\sqrt{2\rho\mu\omega}}{\pi b^2} \left(2 + \frac{d}{b} \right), \quad (2)$$

where μ is the coefficient of viscosity, ω is the angular frequency of an incident wave and d is the orifice thickness. Thus, the relation between the velocity amplitude V_0 and the amplitude $|\hat{P}_i|$ of the driving pressure can be written as

$$V_0 = \frac{2|\hat{P}_i|}{\pi b^2 \sqrt{(R_r + R_t)^2 + X^2}}, \quad (3)$$

where $R_r = \rho c / (\pi a^2)$ is the radiation resistance, $R_t = R_n + R_\mu$ is the total loss resistance and X is the reactance of the resonator.

The theoretical considerations in Part I have indicated that the reactance X may vary as the amplitude of the driving pressure increases. This is a result of a jet contraction and a change in a co-vibrating mass on the outflow side of the resonator orifice. The variation in X has not any influence on the absorption coefficient of resonators and only causes a shift in the resonance frequency, then, due to the lack of an accurate formula for the reactance X at high amplitudes, we decide to use in calculations the expression for X derived from the linear theory

$$X = \frac{\rho c}{\pi a^2} \cot(kl) - k \frac{\rho c}{\pi b^2} (d + \Delta d), \quad \Delta d = \sum_{n=1}^{\infty} \frac{8a J_1^2(\gamma_{0n} b/a)}{\gamma_{0n}^3 J_0^2(\gamma_{0n})}. \quad (4)$$

where Δd is the total end correction for a typical resonator geometry, in which the ratio l/a is not too small ($l/a \geq 1/2$), and γ_{0n} is the n -th root of the equation $dJ_0(\gamma)/d\gamma = 0$.

2.1. Measurement and calculation of absorption coefficient and impedance of resonator

The modulus of the pressure inside the tube in a far field area, according to Part I, is given by

$$|\hat{P}_t| = |\hat{P}_i| \sqrt{1 + \beta^2 + 2\beta \cos(2kz - \chi)}, \quad z \leq 0, \quad (5)$$

where β and χ represent a modulus and a phase of complex reflection coefficient

$$\hat{\beta} = \beta e^{j\chi} = 1 - \frac{2R_r}{R_r + R_t + jX}. \quad (6)$$

The expression for the absorption coefficient α , derived from Eqs. (5) and (6), has a form

$$\alpha = \frac{4|\hat{P}_t|_{\min} |\hat{P}_t|_{\max}}{\left[|\hat{P}_t|_{\min} + |\hat{P}_t|_{\max} \right]^2} = \frac{4R_r R_t}{(R_r + R_t)^2 + X^2}. \quad (7)$$

The first part of Eq. (7) enables to determine α by measurements of minimum and maximum values of standing wave pressure inside the tube, while the second part of it with Eqs. (1)–(4) makes possible a numerical calculation of absorption coefficient (Eq. (3) represents an implicit function of V_0).

An expression for the experimental determination of an impedance of resonator may be easily obtained from Eq. (6). After rearrangement, one can write this equation as

$$R_t + jX = R_r(1 + \hat{\beta})/(1 - \hat{\beta}). \quad (8)$$

If L denotes a distance along z -axis from the first nodal point inside the tube to the orifice plate, then it results from Eq. (5) that

$$\chi = -2kL - \pi. \quad (9)$$

Putting Eq. (9) into Eq. (8) gives finally

$$R_t/R_r = \frac{1 - \beta^2}{1 + \beta^2 + 2\beta \cos(2kL)}, \quad (10)$$

$$X/R_r = \frac{2\beta \sin(2kL)}{1 + \beta^2 + 2\beta \cos(2kL)}. \quad (11)$$

2.2. Experimental prediction of velocity amplitude in resonator orifice

It has been shown in Part I that a pressure in the resonator cavity is uniform in a small distance from the orifice plane, because it represents a superposition of multiple plane wave reflections. The formula for the pressure \hat{P}_l on the rigid plate closing the resonator cavity is thus given by

$$\hat{P}_l(t) = \rho \frac{\partial}{\partial t} \int_0^{2\pi} \int_0^b V_0 e^{-j\omega t} g_c(z_0 = 0, z = l) r_0 dr_0 d\phi_0, \quad (12)$$

where (r_0, ϕ_0, z_0) is a position of the source point in the cylindrical coordinates and $g_c(z, z_0)$ represents Green's function for the plane wave motion inside the resonator cavity

$$g_c(z, z_0) = -\frac{\cos(kz_0)[\sin(kz) + \cos(kz) \cot(kl)]}{k\pi a^2}. \quad (13)$$

After substituting Eq. (13) into Eq. (12) and using the approach $\sin(kl) \approx kl$, which is valid at low frequencies, one can obtain

$$V_0 = \frac{2\pi a^2 fl}{\rho c^2 b^2} |\hat{P}_l|, \quad (14)$$

where $f = \omega/2\pi$ is the frequency of an incident wave. As can be seen, the use of Eq. (14) enables to predict the velocity amplitude V_0 by a measurement of the pressure amplitude $|\hat{P}_l|$ at the closed end of the resonator.

3. Experimental arrangement and apparatus

The tests were carried out by use of the measuring system consisting of a 4002 B&K tube 1 m long and a radius $a = 4.95$ cm, the PW-12 ZOPAN decade generator, the 2712 B&K power amplifier and the 2033 B&K narrowband spectrum analyser (Fig. 2). The 4002 standing wave apparatus permitted a plane wave shape, radiated by the loudspeaker over the frequency range 90–1800 Hz, to be obtained. The resonators located at the end of the tube had the form of a cylindrical chamber with the same radius a as the tube and the length $l = 2.5$ cm. A sharp-edged circular orifice of resonators had the thickness $d = 2$ mm and the radius b from 1 to 3.5 mm.

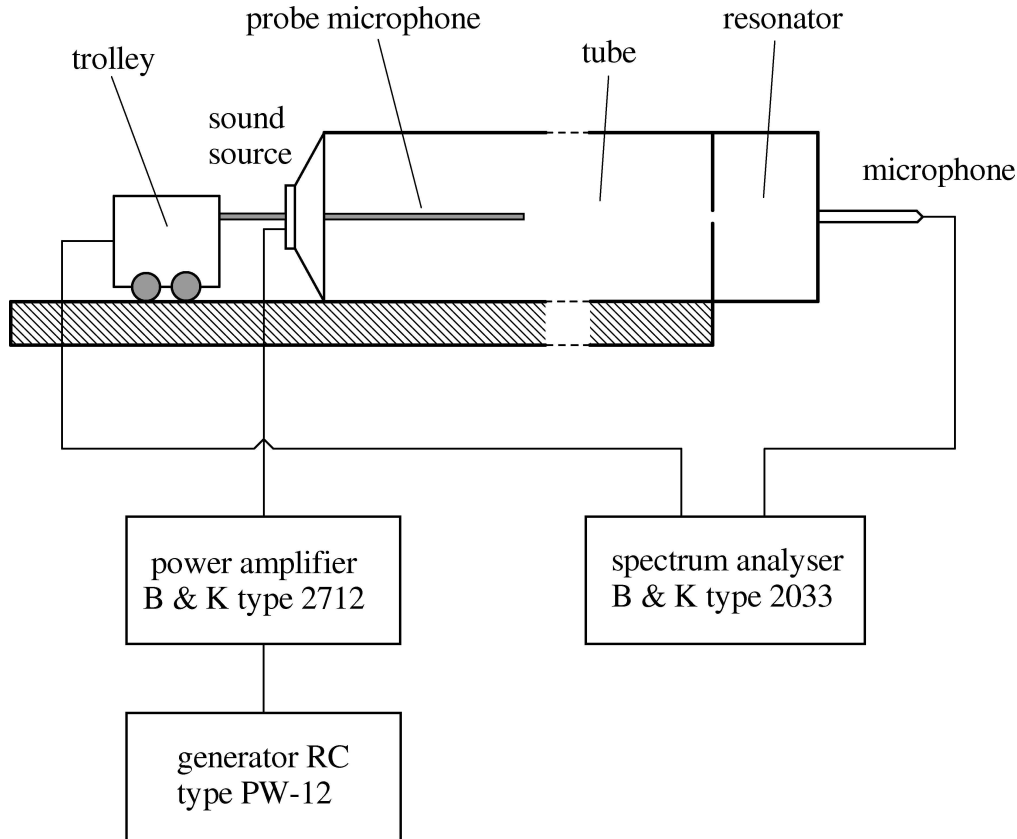


Fig. 2. Setup for measuring the absorption coefficient and impedance of resonator.

The first part of the tests contained measurements of the absorption coefficient α of resonators, in a range of frequencies comprising the fundamental resonance frequency f_{res} , at a constant amplitude $|\hat{P}_i|$ of driving pressure. This condition may be realized experimentally by putting $|\hat{P}_t|_{\text{min}} + |\hat{P}_t|_{\text{max}} = \text{const.}$, because as follows from Eq. (5)

$$|\hat{P}_i| = (|\hat{P}_t|_{\text{min}} + |\hat{P}_t|_{\text{max}})/2. \quad (15)$$

The aim of the tests was to investigate the changes of α in the range of moderate and high amplitudes of driving pressure ($|\hat{P}_i| = 0.11 - 20$ Pa) for resonators with the orifice radius $b = 1.5, 2.5$ and 3.5 mm, and a comparison between experimental and calculation results (Eqs. (1)–(4), (7)). In the second part of the tests, measurements of the total loss resistance R_t and reactance X of the resonator were made for a constant pressure amplitude $|\hat{P}_i|$. In order to measure $|\hat{P}_i|$ an additional slotted line was used with $1/8''$ B&K microphone mounted at the closed end of the resonator (Fig. 2). The purpose of the tests, carried out for resonators with the orifice radius $b = 1, 1.5, 2, 2.5$ and 3.5 mm, was to make a comparison between results of resistance R_t calculations based on the pressure $|\hat{P}_i|$ of incident wave (Eqs. (1)–(4)) and pressure $|\hat{P}_i|$ at the closed end of resonator (Eqs. (1), (2), (14)).

4. Comparison between experimental and calculation results

4.1. Dependence of absorption coefficient α on pressure amplitude of incident wave

The results of measurements are collected in Figs. 3–5, showing the influence of the pressure amplitude $|\hat{P}_i|$ on the absorption coefficient α in the frequency ranges comprising f_{res} . It results from the experimental data that an effect of nonlinearity on coefficient α is the strongest one for the resonator with the orifice radius $b = 1.5$ mm. For the smallest amplitude of driving pressure, $|\hat{P}_i| = 0.11$ Pa, the coefficient α equals 0.85 at the resonance frequency $f_{\text{res}} \approx 160$ Hz (Fig. 3a). It follows from the theoretical part that in this case the total loss resistance, being a sum of the velocity dependent nonlinear resistance R_n and the viscous loss resistance R_μ , is approximately twice as large as the radiation resistance R_r (see Eq. (7)). At the amplitude $|\hat{P}_i|$ much bigger than 0.11 Pa the values of α fast decrease around the resonance frequency (Fig. 3b). It results from a growth in the velocity amplitude V_0 at the resonator orifice which involves an increase of losses due to nonlinearity. Finally, at the highest amplitude of driving pressure, $|\hat{P}_i| = 20$ Pa, the diminution of α takes place below the value of 0.3 in the whole frequency range (Fig. 3c).

A similar character of changes in the absorption coefficient α in the function of the pressure amplitude $|\hat{P}_i|$ has been obtained for the resonators with higher orifice radius. However, in these cases the effect of the driving pressure on the coefficient α is weaker than in the case $b = 1.5$ mm, because for the orifice radius $b = 2.5, 3.5$ mm and $|\hat{P}_i|$ from the range 0.11–20 Pa the maximal values of α change from 0.99 to 0.58 (Fig. 4) and from 0.93 to 0.66 (Fig. 5). The weaker influence of $|\hat{P}_i|$ on the absorption coefficient at higher values of b has a theoretical explanation. As can be seen from Eq. (1), it is a result of the inversely proportional dependence of the nonlinear resistance R_n on the area of the orifice.

The best convergence between experimental and theoretical data can be observed in the case of small values of $|\hat{P}_i|$ when a dependence of α on the frequency f is almost symmetrical around the resonance frequency. There is less agreement between measurements and calculations at the highest amplitude of driving pressure because of an irregularity of

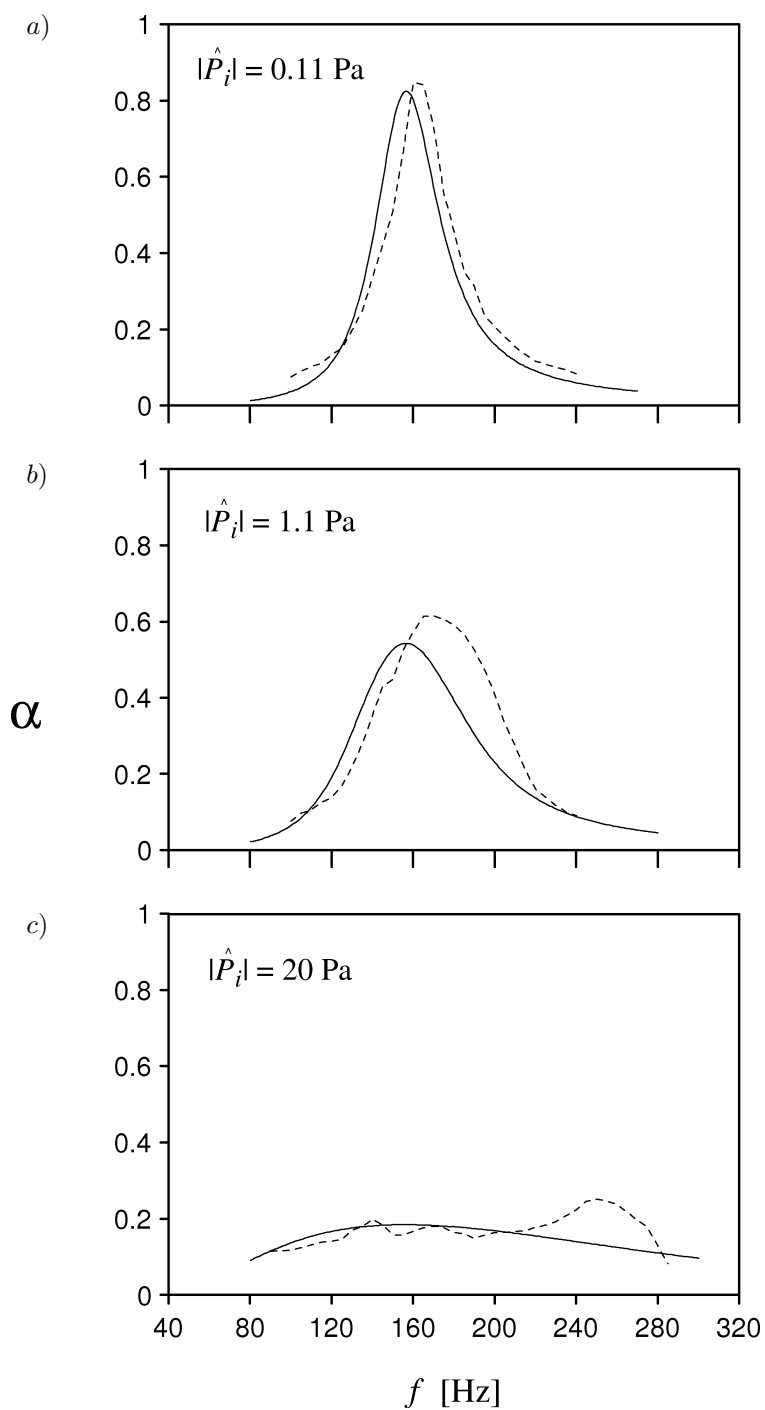


Fig. 3. Frequency dependence of the absorption coefficient α for resonator with orifice radius $b = 1.5$ mm at different pressure amplitudes $|\hat{P}_i|$ of incident plane wave; (- - -) experiment, (—) calculation.

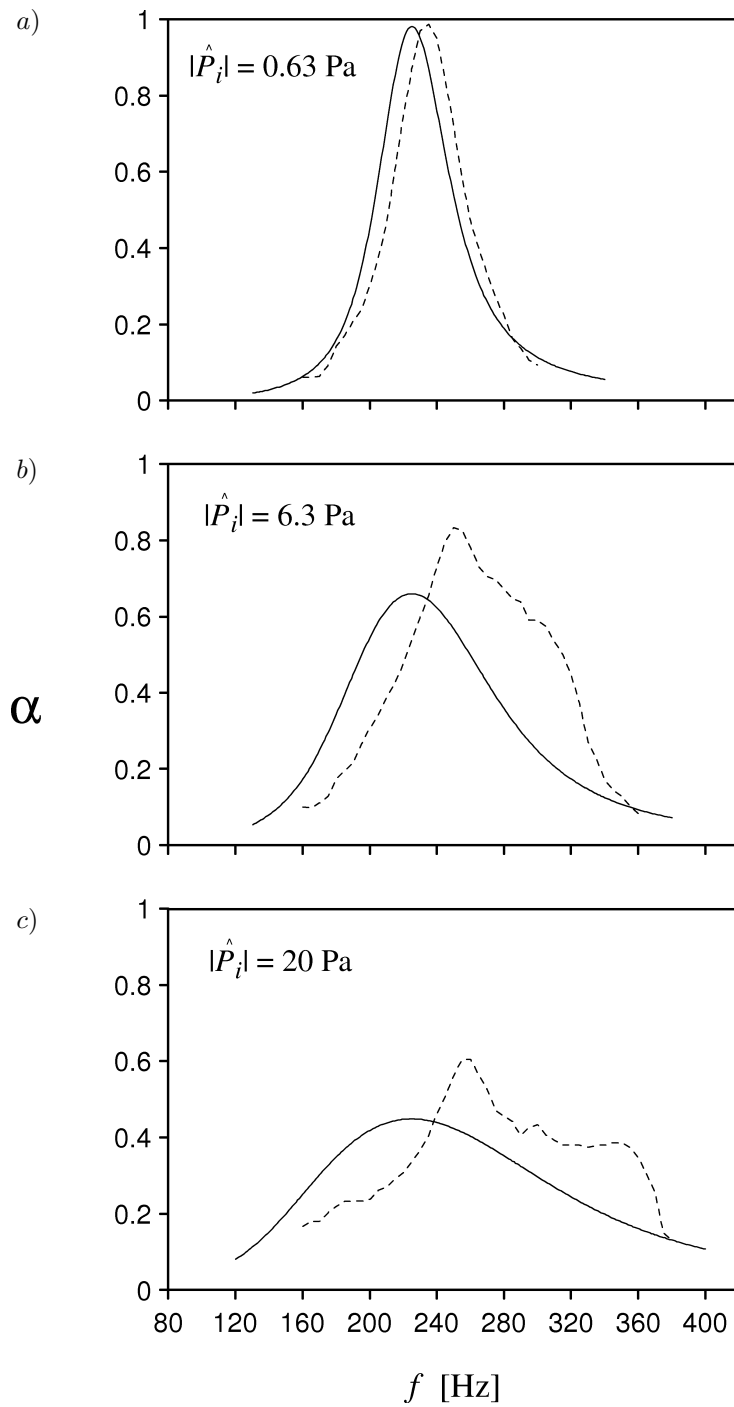


Fig. 4. Frequency dependence of the absorption coefficient α for resonator with orifice radius $b = 2.5$ mm at different pressure amplitudes $|\hat{P}_i|$ of incident plane wave; (- - -) experiment, (—) calculation.

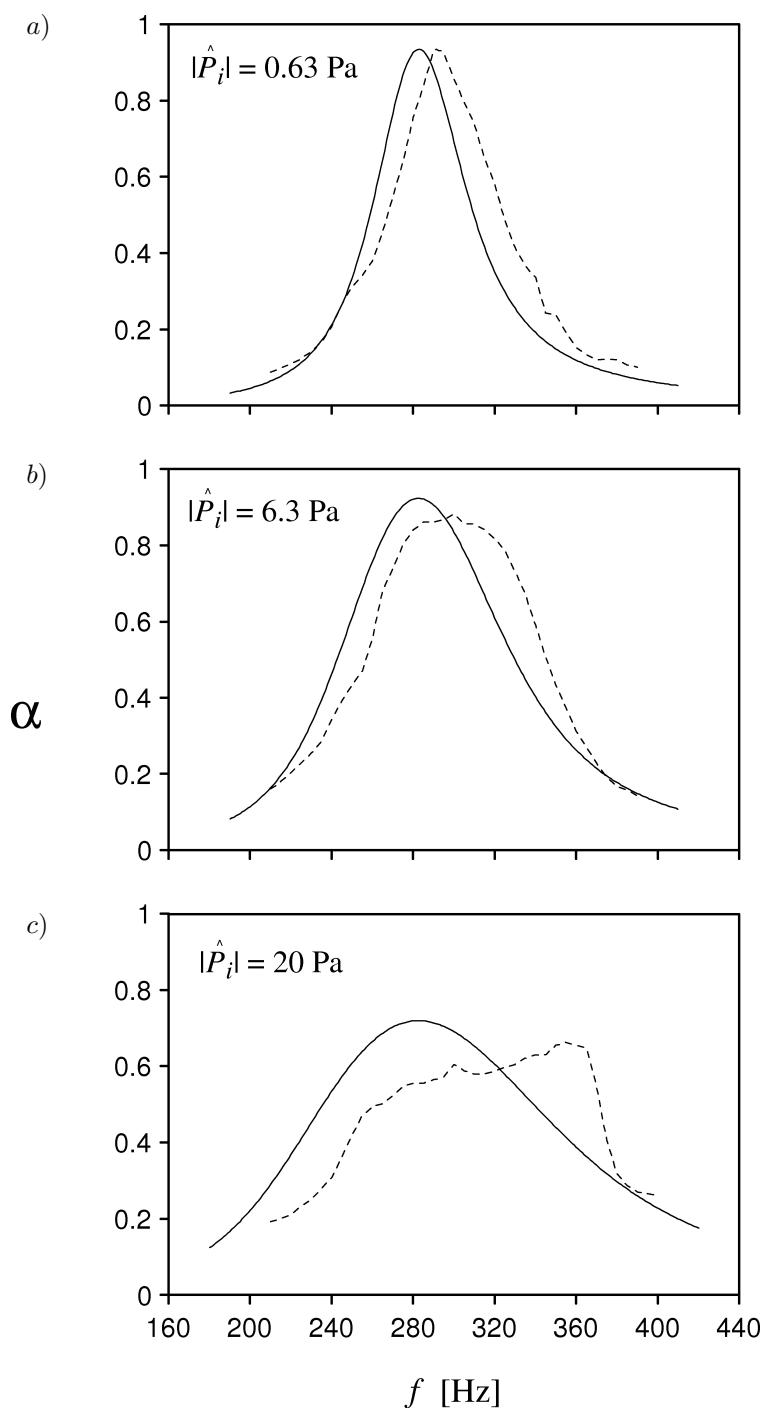


Fig. 5. Frequency dependence of the absorption coefficient α for resonator with orifice radius $b = 3.5$ mm at different pressure amplitudes $|\hat{P}_i|$ of incident plane wave; (- - -) experiment, (—) calculation.

experimental data changes (Figs. 4b, 4c, 5c). This special dependence of α in the function of f can be explained considering the measuring tube as an additional resonance system closed at one end by the resonator and at the other one by the loudspeakers. As a result of mutual interaction between a sound source and a resonator the changes in mechanical parameters of loudspeaker and acoustic properties of resonator take place [11]. This interaction is the most effective in the case of a high sound intensity and resonance in the tube. It can be clearly observed comparing curves in Figs. 4b, 4c, 5c and the plot in Fig. 6, which exhibits an acoustic response of the measuring tube closed by a rigid surface to the white noise. As may be seen, the local maxima of α occur near resonance frequencies of the tube.

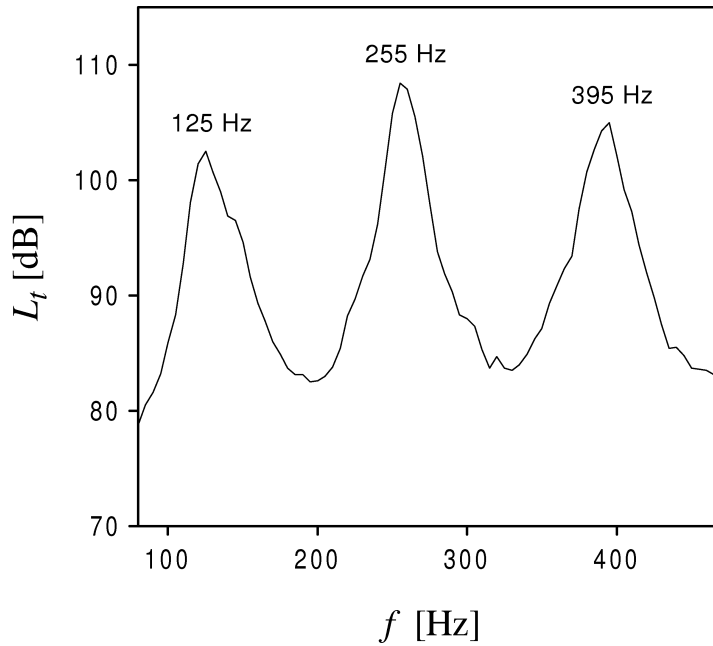


Fig. 6. Frequency dependence of sound pressure level L_t inside the measuring tube closed by a rigid wall in the case of white noise excitation.

4.2. Dependence of resistance R_t on pressure amplitude at closed end of resonator

Equation (14) indicates that a relation between the ratio V_0/f and the pressure $|\hat{P}_l|$ is directly proportional. From this formula and a definition of the total loss resistance the following relationship can be derived

$$\frac{R_t f_{\text{res}}}{R_r f} = \frac{R_\mu f_{\text{res}}}{R_r f} + \frac{\pi l f_{\text{res}} |\hat{P}_l|}{1.23 \rho c^3} \left(\frac{a^2}{b^2 C_c} - 1 \right)^2, \quad (16)$$

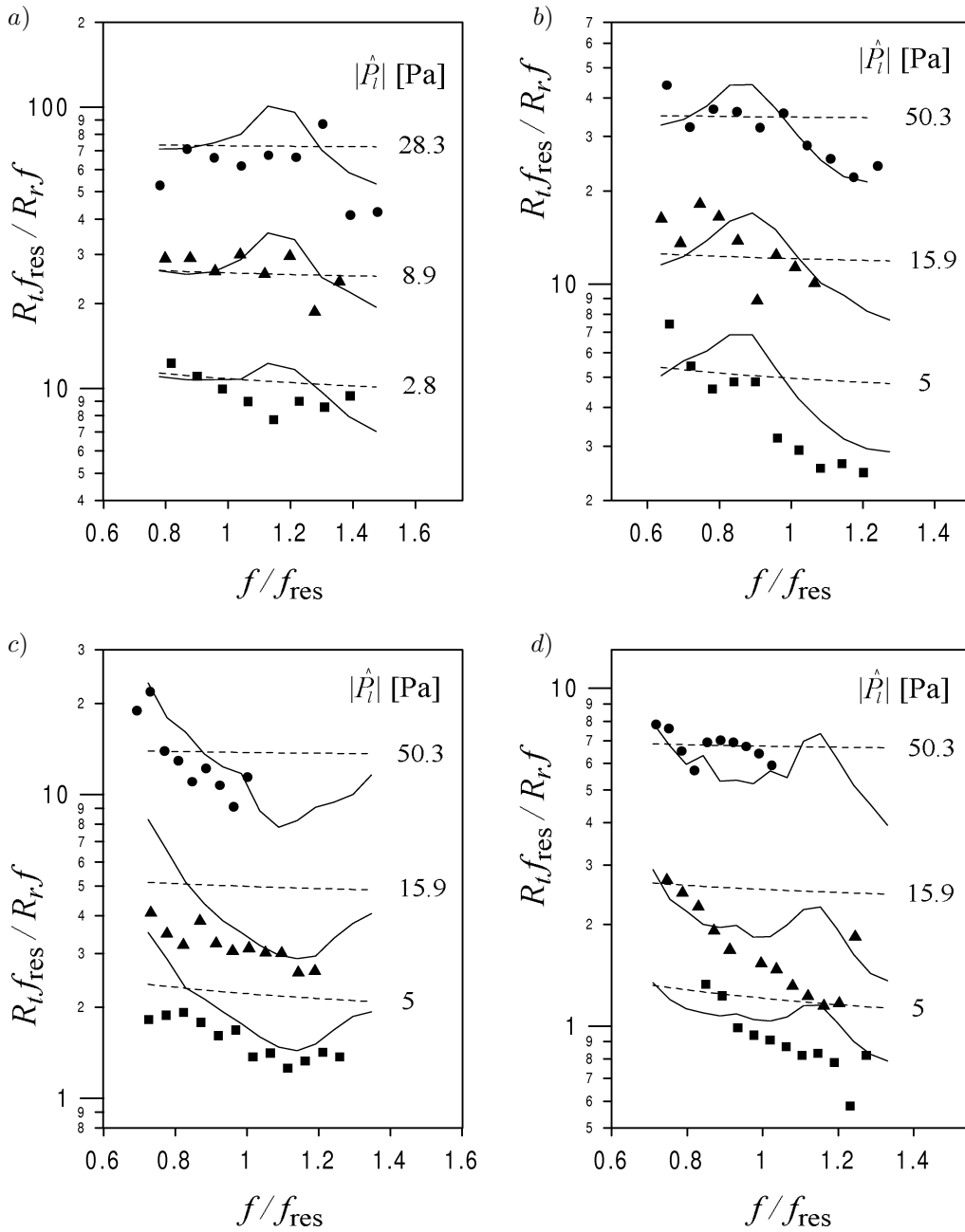


Fig. 7. Changes in $R_t f_{res} / R_r f$ ratio versus nondimensional frequency f / f_{res} at different pressure amplitudes $|\hat{P}_i|$ for resonators with orifice radius b : a) 1 mm, b) 1.5 mm, c) 2 mm, d) 2.5 mm; circles, triangles and squares denote experimental data, (—) calculation results based on amplitude $|\hat{P}_i|$, (- - -) calculation results based on amplitude $|\hat{P}_i|$.

therefore, in the high nonlinear regime ($R_n \gg R_\mu$) the quantity $R_t f_{\text{res}}/R_r f$, for the given dimensions of resonator, approximately assumes the same values at the constant pressure amplitude $|\hat{P}_l|$. Figure 7 shows the experimentally and theoretically determined values of $R_t f_{\text{res}}/R_r f$ in a function of nondimensional frequency f/f_{res} for the pressure $|\hat{P}_l|$ from the range 2.8–50.3 Pa. The fundamental frequency f_{res} of the resonators was evaluated from experimental data or calculated from the condition $X = 0$. In this way, differences between the values of f_{res} obtained from measurements and theory were taken into account in the results presented in Fig. 7.

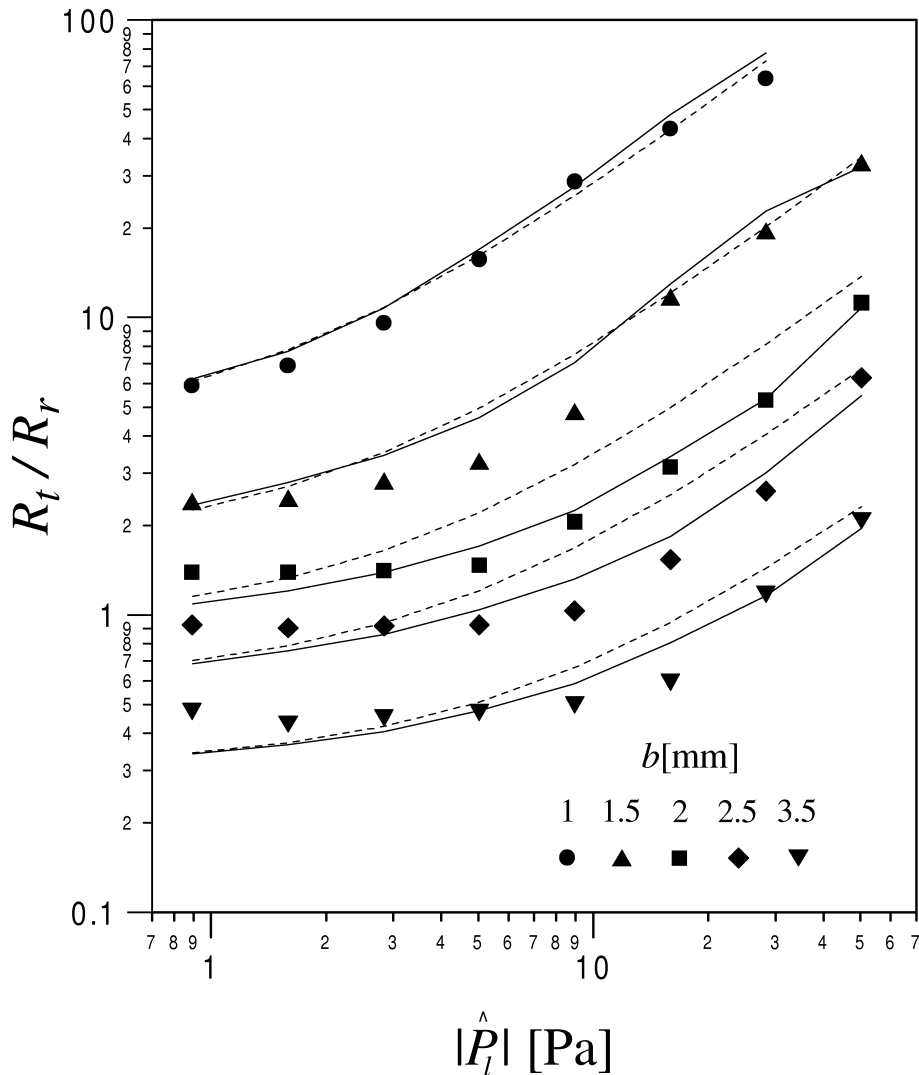


Fig. 8. Dependence of R_t/R_r ratio at resonance frequency on pressure amplitude $|\hat{P}_l|$ for resonators with different orifice radius; (—) calculation results based on amplitude $|\hat{P}_i|$, (- - -) calculation results based on amplitude $|\hat{P}_l|$.

As it was well predicted by theory, the nondimensional parameter $R_t f_{\text{res}}/R_r f$ increases with the pressure amplitude and depends strongly on the orifice radius b . The relation between the quantity $R_t f_{\text{res}}/R_r f$ and the orifice radius b , which results from experimental data, can be simply defined: a smaller value of b — a higher value of $R_t f_{\text{res}}/R_r f$ at the same amplitude $|\hat{P}_l|$. A more precise description of this dependence is possible in the case of resonance ($f/f_{\text{res}} = 1$), when the agreement between measurements and data computed from Eq. (15) is satisfactory (in Fig. 7 indicated by dashed lines). For other values of f/f_{res} , results of calculations based on the pressure amplitude $|\hat{P}_l|$ of incident wave (in Fig. 7 indicated by solid lines) approximate better the experimental data.

In order to illustrate a more general dependence between total resistance and pressure amplitude $|\hat{P}_l|$, the changes in $R_t f_{\text{res}}/R_r f$ values for resonance frequencies ($f/f_{\text{res}} = 1$) in a function of $|\hat{P}_l|$ are shown in Fig. 8. It is evident from Fig. 8 that for each resonator the calculation results and the experimental data are in close agreement in a range of $|\hat{P}_l|$ where the energy loss is dominated by the nonlinear absorption. In the case of resonator with the smallest orifice radius this range covers almost all values of $|\hat{P}_l|$ used in the experiment. Larger differences are observed for the resonators with higher orifice dimensions. In the ranges of $|\hat{P}_l|$, where the theory is less accurate, the energy loss is due to the nonlinearity and the viscous damping. In a theoretical model this damping was described by resistance R_μ (Eq. (2)) and, as may be seen in Fig. 8, a calculated value of R_μ is somewhat smaller than an experimental one.

4.3. Dependence of reactance X on pressure amplitude at closed end of resonator

An increase in the total loss resistance of Helmholtz resonators is not only unique result of acoustic nonlinearity. The second effect of this phenomenon is a change in the resonator reactance with growing sound intensity. A precise theoretical description of this effect is difficult, therefore in the impedance model of a resonator (presented in Sec. 2) the reactance X was determined by Eq. (4) as in the case of linear theory.

The experimental data shown in Fig. 9 illustrate the changes in nondimensional reactance X/R_r as a function of frequency f for different values of pressure amplitude $|\hat{P}_l|$. The values of X/R_r calculated from Eq. (4) are indicated by solid lines. As may be seen from Fig. 9, there is a good agreement between theory and experiment at the moderate pressure amplitudes $|\hat{P}_l| = 1.6, 5 \text{ Pa}$. At much higher values of $|\hat{P}_l|$ an increase of the reactance X is observed but it is different for various resonators. The least modification of the reactance can be noted for the resonator with the highest orifice radius (Fig. 9d). For other resonators the changes in X versus frequency at high values of $|\hat{P}_l|$ may appear without any regularity (Fig. 9a) or have almost regular shape (Figs. 9b, 9c). As a result of the increase in the reactance it appears a shift in resonance frequency to higher frequencies which is clearly observed for resonators with the orifice radius $b = 2$ and 2.5 mm at the highest pressure amplitude $|\hat{P}_l|$ (Figs. 9b, 9c).

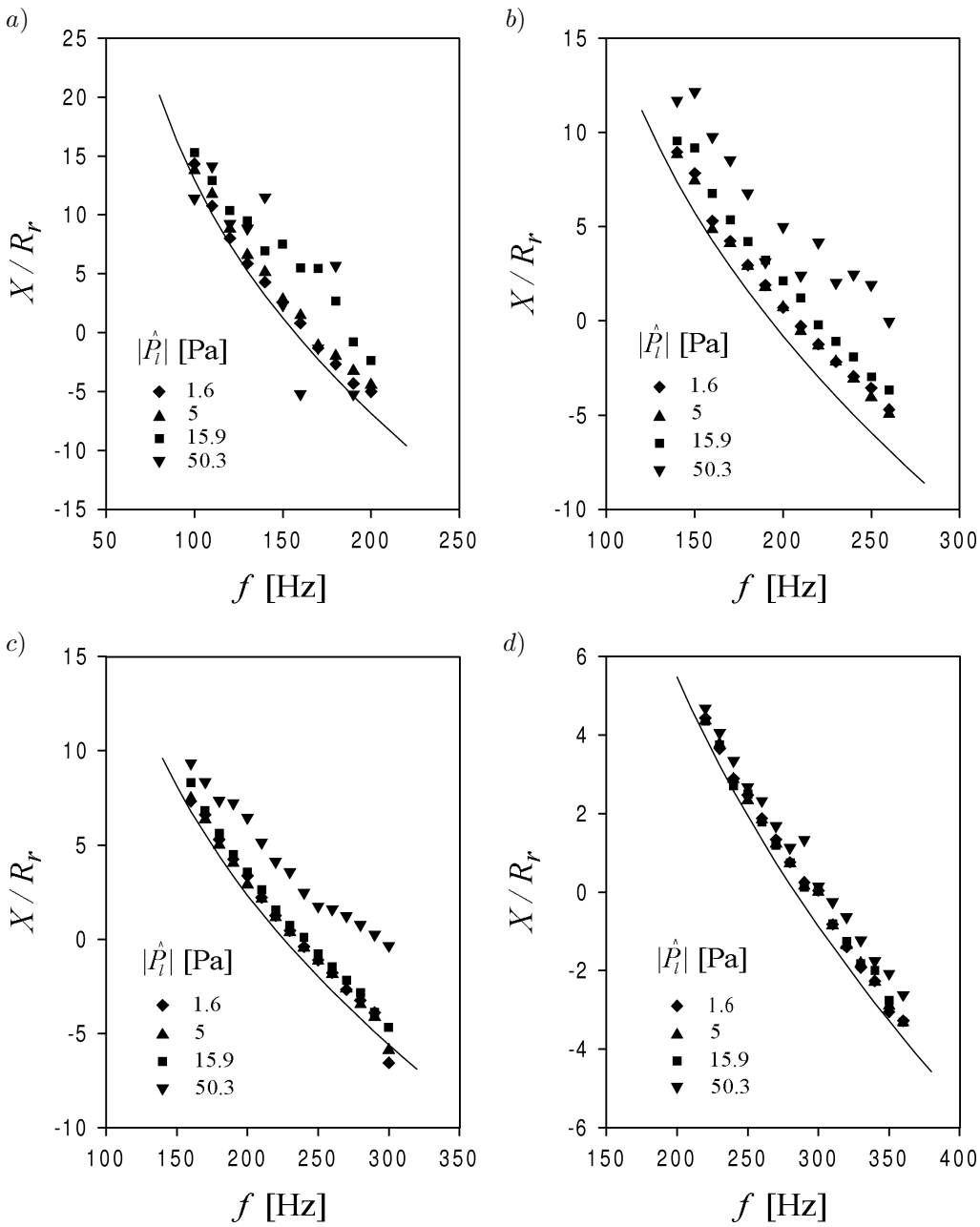


Fig. 9. Changes of nondimensional reactance X/R_r versus frequency f at different pressure amplitudes $|\hat{P}_l|$ for resonators with orifice radius b : a) 1.5 mm, b) 2 mm, c) 2.5 mm, d) 3.5 mm; (—) calculation results.

5. Conclusions

The experimental results presented in this paper have demonstrated the effect of nonlinearity on acoustic properties of Helmholtz resonators. The most important aspect of this phenomenon is a change in the absorption coefficient α at the high sound intensities. The measurements performed under condition of constant amplitudes $|\hat{P}_i|$ of driving pressure have shown that for a small diameter of the resonator orifice an influence of nonlinearity may be very strong because it results in an increase in α to value near unity at a resonance frequency even at moderate pressure amplitudes (Figs. 4a, 5a). In the case of much higher pressures, as it was predicted by the theory, the observed decrease in α was evidently larger for a smaller orifice diameters (Figs. 3c, 4c, 5c).

According to the theory developed in Part I, a change in α with the sound intensity is connected with an increase of nonlinear resistance. It was confirmed by results of resistance R_t measurements which were performed under condition of constant amplitude $|\hat{P}_l|$ of pressure at the closed end of resonator. A comparison between experimental data and calculation results has proved that at high values of $|\hat{P}_l|$ a relation between the resistance R_t and the pressure amplitude $|\hat{P}_l|$ at the resonance frequency may be approximated by Eq. (15). The agreement between measurements and theory was worse in the range of low values of $|\hat{P}_l|$ when energy absorption is dominated by viscous damping (Fig. 8).

In the presented theory a reactance of Helmholtz resonators has been described as a part of the impedance which is independent of the amplitude of incident wave. A change in the reactance has no influence on absorption properties of resonators but it may cause an increase in the resonance frequency. It appears that the reactance is much less sensitive than the resistance to changes in sound intensity because a shift in the resonance frequency to higher frequencies was clearly observed only at the highest pressure amplitude $|\hat{P}_l|$ (Fig. 9).

References

- [1] F.J. FAHY and C. SCHIFIELD, *A note on the interaction between a Helmholtz resonator and an acoustic mode of an enclosure*, J. Sound Vib., **72**, 3, 365–378 (1980).
- [2] H.L. KUNTZ, R.A. PRYDZ, F.J. BALENA and R.J. GATINEAU, *Development and testing of cabin sidewall acoustic resonators for the reduction of cabin tone levels in propfan-powered aircraft*, Noise Control Engineering Journal, **37**, 3, 129–142 (1991).
- [3] J.M. MASON and F.J. FAHY, *The use of acoustically tuned resonators to improve the sound transmission loss of double-panel partitions*, J. Sound Vib., **124**, 2, 367–379 (1988).
- [4] R.A. PRYDZ, L.S. WIRT, H.L. KUNTZ and L.D. POPE, *Transmission loss of a multilayer panel with internal tuned Helmholtz resonators*, J. Acoust. Soc. Amer., **87**, 4, 1597–1602 (1990).
- [5] U. INGARD, *On the theory and design of acoustic resonators*, J. Acoust. Soc. Amer., **25**, 6, 1037–1061 (1953).
- [6] D.A. BIES and O.B. WILSON, *Acoustic impedance of a Helmholtz resonator at very high amplitude*, J. Acoust. Soc. Amer., **29**, 6, 711–714 (1957).
- [7] J. WU and I. RUDNICK, *Measurements of the nonlinear tuning curves of Helmholtz resonators*, J. Acoust. Soc. Amer., **80**, 5, 1419–1422 (1986).

- [8] S. CZARNECKI, *Utilization of nonlinear properties of resonators for improving acoustic conditions in rooms*, Proceedings of the 6th International Congress on Acoustics, Tokyo, Japan, 197–200 (1968).
- [9] S. CZARNECKI, *Nonlinear absorption properties of acoustic resonance systems* [in Polish], Arch. Akustyki, **1**, 4, 37–49 (1969).
- [10] M. MEISSNER, *The influence of acoustic nonlinearity on absorption properties of Helmholtz resonators. Part I. Theory*, Arch. Acoust., **24**, 2, 179–190 (1999).
- [11] M. MEISSNER, *Mechano–acoustic feedback in the case of an interaction between a sound source and a resonance system*, Arch. Acoust., **8**, 3, 235–248 (1983).